Interpretation of spin-polarized electron energy loss spectra

R. Saniz
Departamento de Ciencias Exactas, Universidad Católica Boliviana, Casilla #5381, Cochabamba, Bolivia

S. P. Apell
Department of Applied Physics, Chalmers University of Technology and Göteborg University, S-41 296, Göteborg, Sweden
(Received 3 March 2000; revised manuscript received 24 August 2000; published 11 December 2000)

We study the origin of the structure in the spin-polarized electron energy loss spectroscopy (SPEELS) spectra of itinerant-electron ferromagnetic crystals. For our study we consider a model based on $3d$ tight-binding energy bands and a multiband Hubbard Hamiltonian. We find it is not the total density of Stoner states that determines the response of the system in the Stoner region, as usually thought, but the densities of Stoner states for only a few interband transitions. Which transitions are important depends ultimately on how strongly umklapp processes couple the corresponding bands. This allows us to show, in particular, that the Stoner peak in SPEELS spectra does not necessarily indicate the value of the exchange-splitting energy. Thus, the common assumption that this peak allows us to estimate the magnetic moment through its correlation with exchange splitting should be reconsidered, both in bulk and surface studies. The above mechanism is also one of the main causes for the typical broadness of experimental spectra. Finally, our model predicts that high-energy spin waves should be excited in SPEELS experiments.

DOI: 10.1103/PhysRevB.63.014409 PACS number(s): 75.30.Ds

I. INTRODUCTION

The study of elementary excitations in itinerant-electron ferromagnets is an area that is currently very active in spite of the enormous amount of publications on the subject since early work in the 1960s (see, e.g., Refs. 1 and 2 and references therein). From the beginning, experimental and theoretical work on these materials concentrated on neutron scattering and dynamical susceptibility studies.[1,3–6] Efforts have continued in this direction until today, both because of the gradual improvement of electronic band-structure calculations[7,8] and because of the improvement of the experimental method.[9] Around the mid-1980s, however, a new technique was introduced in the field, namely, spin-polarized electron energy loss spectroscopy (SPEELS). Among its first successes, one can count the first observations, in a ferromagnetic glass[10] and in nickel,[11] of what were interpreted as Stoner excitations, i.e., electron-hole pairs with electrons and holes of opposite spin. Further work, reporting more detailed measurements, confirmed those findings.[12,13] Theoretical model calculations of inelastic electron spin-flip exchange scattering[14–17] provided a basis for the interpretation of those observations in terms of Stoner excitations. In addition, Vignale and Singwi found in their work that spin waves should also be observable in SPEELS measurements.[16] These had not been observed at the time, however, nor were they observed in the several years that followed. Spin waves were found in other model SPEELS calculations,[18,19] the ones by Plihal and Mills being the most conclusive in this respect because of their more accurate treatment of electronic structure.[19] It is only very recently that the detection of spin waves in a SPEELS experiment has finally been reported.[20] The application of SPEELS has been naturally extended to the study of magnetic surfaces.[21–23] An important theoretical effort in this direction is that by Mills and collaborators,[24–26] who have studied ferromagnetic thin films as well.

To introduce the questions addressed by this work, we recall briefly some of the main concepts involved in SPEELS and discuss some of the findings to date. SPEELS is a spin-polarized version of electron energy loss spectroscopy in the sense that the spin polarization of the scattered electrons is also measured. The impinging electron often is also spin polarized, but this is not necessarily so (see, e.g., Refs. 10 and 11). In a so-called spin-flip exchange scattering event, an incoming electron with given spin comes to occupy an empty level in the material, while an electron with opposite spin is driven out and is detected. The process thus produces a Stoner excitation. In the band picture of magnetic transition metals, below the Curie temperature, the exchange split $3d$ bands provide large densities of occupied majority-spin states below the Fermi energy and vacant minority-spin states above it. Thus, it is more likely for an impinging electron with minority spin to excite a Stoner pair than for a majority-spin incoming electron, particularly for an excitation energy corresponding to the exchange splitting of the ferromagnet. This is the mechanism invoked to explain the Stoner peak or the asymmetry reported in Refs. 10 and 11 and further experimental work (Refs. 12 and 13). However, it turned out necessary to elaborate on several other issues. First, the Stoner peak was very broad in all observations. This was interpreted by Kirschner, Rebenstorff, and Ibach[11] as an indication of the nonuniformity of exchange splitting throughout the Brillouin zone. Then, in Fe, the energy loss at which the Stoner peak occurs and its width were reported by Venus and Kirschner to increase with increasing scattering angle,[12] a fact that was correlated by these authors with the calculated density of Stoner states. Also, a threshold for the onset of Stoner excitations in Ni(110) was reported by Abraham and Hopster[13] and interpreted in terms of the Ni $3d$ band structure. These workers, moreover, indicated that their spectra did not differ significantly for off specular scattering angles ranging from 10° to 40°,[27] which they explained as

due to the nonconservation of the momentum component perpendicular to the surface.

Finally, an important application based on SPEELS interpretation is that, in surface and thin-film studies, the Stoner peak is assumed to give information on the surface magnetic moment through the correlation between exchange splitting and moment.[22,23] In particular, a Stoner peak found at higher energies than the exchange splitting bulk value is assumed to indicate an enhanced magnetic moment at the surface.

Clearly, more theoretical work is required, for the bulk as much as for surfaces, to make further progress. In particular, it would be important to understand better the phenomenology of SPEELS and to try to be more specific about the information we can expect from it. This would also provide experimenters with useful feedback. Accordingly, we think it is worthwhile going back to a model calculation and look more closely at the dynamic properties of the material probed by SPEELS. In this work we consider a model of an itinerant-electron ferromagnet based on paramagnetic tight-binding $3d$ bands, assuming the interacting system is described by a multiband Hubbard Hamiltonian. The effective on-site Coulomb repulsion U between electrons of opposite spin is taken constant. The cross section for spin-flip exchange scattering processes is evaluated within the random-phase approximation (RPA). As we shall see, this allows us to show that it is not the total density of Stoner states as a function of energy loss and momentum transfer that causes the structure in the Stoner region of the spectrum, but the density of Stoner states for a few interband excitations. Which interband excitations are important is essentially determined by the weight of the matrix elements for such processes. In this regard the contribution of umklapp scattering is fundamental because of the coupling of different bands at different energy ranges. This gives rise to a richer structure in the Stoner region of the spectra. Also, our model predicts that the high-energy spin waves reported in the past in neutron scattering studies[9,28–30] should be observable through SPEELS as well. Again, umklapp scattering proves critical, providing enough coupling between the impinging electron and those in the solid to excite these spin waves.

Section II of this paper is devoted to theory, presenting the derivation of the spin-flip exchange scattering cross section for our model. We present our main results in Sec. III. Then follows, in Sec. IV, a discussion of our results in the light of experimental findings and other theoretical work. Finally, in Sec. V, we summarize our work and give some conclusions.

II. THEORY

A. Spin-flip exchange scattering cross section

The electron spin-flip exchange scattering differential cross section for an N-electron system target has been previously derived on general grounds by Vignale and Singwi in terms of a particle-hole excitation correlation function.[16] One has

$$\frac{d^2\sigma}{dE\,d\Omega}=-\frac{m^2}{4\pi^2\hbar^4}\frac{p_f}{p_i}\frac{1}{\pi}\frac{\mathrm{Im}\,\chi^R_{\sigma_i\sigma_f}(\mathbf{p}_i,\mathbf{q},E)}{1-e^{-\beta E}}, \tag{2.1}$$

where E is the energy loss, Ω is the solid angle, m is the electron mass, and $\beta=1/k_BT$. Momentum transfer is given by $\mathbf{q}=\mathbf{p}_i-\mathbf{p}_f$, with $\mathbf{p}_i$ and $\mathbf{p}_f$ the momentum of the incoming and outgoing electrons, respectively. Likewise, σ_i is the spin of the impinging electron and σ_f is the spin of the scattered one. The retarded function $\chi^R_{\sigma_i\sigma_f}$ can be obtained by analytic continuation of the two-particle temperature correlation function

$$\chi_{\sigma_i\sigma_f}(\mathbf{p}_i,\mathbf{q},i\omega_n)=-\int_0^\beta d\tau\, e^{-i\omega_n\tau}\times\langle T_\tau[\varrho_{\sigma_i\sigma_f}(\mathbf{p}_i,\mathbf{q},\tau)\varrho^\dagger_{\sigma_i\sigma_f}(\mathbf{p}_i,\mathbf{q})]\rangle. \tag{2.2}$$

In this equation $\omega_n=2\pi n/\beta$ is a bosonic Matsubara frequency, T_τ is the imaginary time ordering operator, and the angular brackets indicate the thermodynamic average in the canonical ensemble.[31] $\varrho^\dagger_{\sigma_i\sigma_f}$ is the particle-hole creation operator

$$\varrho^\dagger_{\sigma_i\sigma_f}(\mathbf{p}_i,\mathbf{q})=-\frac{1}{N}\sum_{j=1}^{N}\int d\mathbf{r}\,d\mathbf{r}_j e^{-i\mathbf{p}_f\cdot\mathbf{r}_j}e^{i\mathbf{p}_i\cdot\mathbf{r}}v(|\mathbf{r}-\mathbf{r}_j|)\times\psi^\dagger_{\sigma_i}(\mathbf{r})\psi_{\sigma_f}(\mathbf{r}_j), \tag{2.3}$$

where $\psi^\dagger_\sigma(\mathbf{r})$ is the field operator creating an electron of spin σ at position $\mathbf{r}$ and $v(r)=e^2/r$ is the Coulomb interaction between the scattered and target electrons. The sum runs over the N electrons in the target system. This expression is quite general and could be applied equally well to a solid, an atom, or a molecule.

We now consider the N electrons in a crystal material. We write the Bloch wave function for a state with wave vector $\mathbf{k}$ and spin σ in band n in terms of Wannier functions:

$$\psi_{n\mathbf{k}\sigma}(\mathbf{r})=\frac{1}{\sqrt{N_0}}\sum_{\mathbf{R}}e^{i\mathbf{k}\cdot\mathbf{R}}\phi_{n\mathbf{k}}(\mathbf{r}-\mathbf{R})\,\eta_\sigma, \tag{2.4}$$

where N_0 is the number of sites in the crystal and η_σ is the spin function. Denoting by $a^\dagger_{n\mathbf{k}\sigma}$ the operator creating an electron in such a state, the field operators can be expanded as $\psi^\dagger_\sigma(\mathbf{r})=\Sigma_{n\mathbf{k}}\psi_{n\mathbf{k}\sigma}(\mathbf{r})a^\dagger_{n\mathbf{k}\sigma}$. The particle-hole creation operator becomes

$$\varrho^\dagger_{\sigma_i\sigma_f}(\mathbf{p}_i,\mathbf{q})=\sum_{nn'}\sum_{\mathbf{k}}W_{nn'}(\mathbf{p}_i,\mathbf{q},\mathbf{k})a^\dagger_{n\mathbf{k}\sigma_i}a_{n'\mathbf{k}-\mathbf{q}\sigma_f}, \tag{2.5}$$

where the sum in momentum space runs over the Brillouin zone, and matrix element $W_{nn'}$ is given by

$$W_{nn'}(\mathbf{p}_i,\mathbf{q},\mathbf{k})=\frac{N_0}{V}\sum_{\mathbf{K}}\hat{v}(\mathbf{k}-\mathbf{p}_i-\mathbf{K})\hat{\phi}^*_{n\mathbf{k}}(\mathbf{k}-\mathbf{K})\times\hat{\phi}_{n'\mathbf{k}-\mathbf{q}}(\mathbf{k}-\mathbf{q}-\mathbf{K}). \tag{2.6}$$

Here, $\mathbf{K}$ denotes vectors in the reciprocal lattice and V is the volume of the sample. The caret indicates a Fourier-

transformed function, and the asterisk denotes complex conjugation. To write the last two equations, we have defined $a_{n\mathbf{k}+\mathbf{K}\sigma} \equiv a_{n\mathbf{k}\sigma}$ and have exploited the periodicity of the Wannier functions in the wave-vector index, i.e., $\phi_{n\mathbf{k}+\mathbf{K}} = \phi_{n\mathbf{k}}$.

B. RPA expression for a tight-binding system

We are interested in the cross section for an itinerant electron ferromagnet. We describe the system within a tight-binding approximation, thus writing the Wannier wave function for given $\mathbf{k}$ and band index n by a linear combination of atomic orbitals φ_m,

$$\phi_{n\mathbf{k}}(\mathbf{r}) = \sum_m b_{mn}(\mathbf{k})\varphi_m(\mathbf{r}). \tag{2.7}$$

The coefficients b_{mn} diagonalize the crystal Hamiltonian and are normalized so as to define a unitary matrix. Consequently, the independent-electron Hamiltonian of the system can be written $H_0 = \Sigma_{n\mathbf{p}\sigma}\epsilon_n(\mathbf{p})a^\dagger_{n\mathbf{p}\sigma}a_{n\mathbf{p}\sigma}$, where the $\epsilon_n(\mathbf{p})$ are paramagnetic band energies. We assume the interacting system is described by the multiband Hubbard Hamiltonian

$$H_I = \frac{1}{2}U\sum_{mm'}\sum_{\mathbf{R}}\sum_{\sigma} n_{m\mathbf{R}\sigma}n_{m'\mathbf{R}-\sigma}, \tag{2.8}$$

where $n_{m\mathbf{R}\sigma}$ is the occupation number of state with spin σ at site $\mathbf{R}$ in orbital m, and U is the effective on-site Coulomb repulsion between electrons with opposite spin. In our Bloch states basis this becomes

$$H_I = \frac{1}{2}\frac{U}{N_0}\sum_{\substack{nn'\\mm'}}\sum_{\mathbf{p}\mathbf{p}'\mathbf{q}'}\sum_{\sigma} c_{nm}(\mathbf{p}+\mathbf{q}',\mathbf{p})c_{n'm'}(\mathbf{p}'-\mathbf{q}',\mathbf{p}') \times a^\dagger_{n\mathbf{p}+\mathbf{q}'\sigma}a_{m\mathbf{p}\sigma}a^\dagger_{n'\mathbf{p}'-\mathbf{q}'-\sigma}a_{m'\mathbf{p}'-\sigma}, \tag{2.9}$$

where we have defined $c_{nm}(\mathbf{p},\mathbf{q}) = \Sigma_l b_{ln}(\mathbf{p})b_{lm}(\mathbf{q})$. The RPA evaluation of the correlation function $\chi_{\sigma_i\sigma_f}$ defined in Eq. (2.2) is a straightforward generalization of that in previous work.[18] The response function divides naturally in two:

$$\chi_{\sigma_i\sigma_f}(\mathbf{p}_i,\mathbf{q},i\omega_n) = \chi^{\mathrm{S}}_{\sigma_i\sigma_f}(\mathbf{p}_i,\mathbf{q},i\omega_n) + \chi^{\mathrm{MB}}_{\sigma_i\sigma_f}(\mathbf{p}_i,\mathbf{q},i\omega_n). \tag{2.10}$$

The Stoner or single-particle excitation contribution is given by

$$\chi^{\mathrm{S}}_{\sigma_i\sigma_f}(\mathbf{p}_i,\mathbf{q},i\omega_n) = \sum_{nn'}\sum_{\mathbf{k}}\frac{f_{n'\mathbf{k}-\mathbf{q}\sigma_f} - f_{n\mathbf{k}\sigma_i}}{i\omega_n + \epsilon_{n'\sigma_f}(\mathbf{k}-\mathbf{q}) - \epsilon_{n\sigma_i}(\mathbf{k})} \times |W_{nn'}(\mathbf{p}_i,\mathbf{q},\mathbf{k})|^2. \tag{2.11}$$

We have introduced the occupation probability of state $n\mathbf{k}\sigma$, $f_{n\mathbf{k}\sigma} = \langle a^\dagger_{n\mathbf{k}\sigma}a_{n\mathbf{k}\sigma}\rangle$, and the single-particle energy modified by the exchange self-energy:

$$\epsilon_{n\sigma}(\mathbf{k}) = \epsilon_n(\mathbf{k}) - \frac{U}{N_0}\sum_{\mathbf{p}} f_{n\mathbf{p}\sigma}. \tag{2.12}$$

Thus, in this model, spin-down and spin-up energy bands are rigidly split by the quantity $\Delta = U(\langle n_\uparrow\rangle - \langle n_\downarrow\rangle)$, where

$$\langle n_\sigma\rangle = \frac{1}{N_0}\sum_{m\mathbf{p}} f_{m\mathbf{p}\sigma} \tag{2.13}$$

is the average number per site of states with spin σ.

The many-body contribution is given by

$$\chi^{\mathrm{MB}}_{\sigma_i\sigma_f}(\mathbf{p}_i,\mathbf{q},i\omega_n) = \frac{U}{N_0}\sum_{nn'} G^{nn'}_{\sigma_i\sigma_f}(\mathbf{p}_i,\mathbf{q},i\omega_n)\Gamma^{nn'}_{\sigma_i\sigma_f}(\mathbf{p}_i,\mathbf{q},i\omega_n), \tag{2.14}$$

with the auxiliary functions $G^{nn'}$ and $\Gamma^{nn'}$ defined as follows:

$$G^{nn'}_{\sigma_i\sigma_f}(\mathbf{p}_i,\mathbf{q},i\omega_n) = \sum_{mm'}\sum_{\mathbf{k}}\frac{f_{m'\mathbf{k}-\mathbf{q}\sigma_f} - f_{m\mathbf{k}\sigma_i}}{i\omega_n + \epsilon_{m'\sigma_f}(\mathbf{k}-\mathbf{q}) - \epsilon_{m\sigma_i}(\mathbf{k})} \times W^*_{mm'}(\mathbf{p}_i,\mathbf{q},\mathbf{k})b_{nm}(\mathbf{k})b_{n'm'}(\mathbf{k}-\mathbf{q}), \tag{2.15}$$

and, considering G and Γ as vectors with coefficients indexed by nn',

$$\Gamma_{\sigma_i\sigma_f}(\mathbf{p}_i,\mathbf{q},i\omega_n) = \left[1 + \frac{U}{N_0}D_{\sigma_i\sigma_f}(\mathbf{q},i\omega_n)\right]^{-1} \times G_{\sigma_i\sigma_f}(\mathbf{p}_i,\mathbf{q},i\omega_n), \tag{2.16}$$

where the elements of matrix D are

$$D^{nn',mm'}_{\sigma_i\sigma_f}(\mathbf{q},i\omega_n) = \sum_{ll'}\sum_{\mathbf{k}} b_{nl}(\mathbf{k})b_{n'l'}(\mathbf{k}-\mathbf{q}) \times \frac{f_{l'\mathbf{k}-\mathbf{q}\sigma_f} - f_{l\mathbf{k}\sigma_i}}{i\omega_n + \epsilon_{l'\sigma_f}(\mathbf{k}-\mathbf{q}) - \epsilon_{l\sigma_i}(\mathbf{k})} \times b_{ml}(\mathbf{k})b_{m'l'}(\mathbf{k}-\mathbf{q}). \tag{2.17}$$

To obtain $\chi^R_{\sigma_i\sigma_f}$, analytic continuation $i\omega_n \to E + i\eta$ of the above results is straightforward. Also, the results in the next section are obtained in the zero-temperature limit.

III. RESULTS

Before presenting our results, there are a few details of our model that we should discuss. First, for definiteness we have taken parameter values corresponding to Fe. Then, as we said in the Introduction, our model is based on simple $3d$ tight-binding paramagnetic bands, i.e., we neglect sp hybridization. This has, of course, consequences on the quantitative details of the response of the system. However, we focus on the qualitative aspects of our results and are thus able to draw conclusions valid generally for itinerant-electron ferromagnets.

The Wannier functions were written as a linear combination of the five $3d$ Fe atomic wave functions. The overlap integrals were calculated, up to next-nearest neighbors, using the Fe atomic wave functions determined according to Grif-

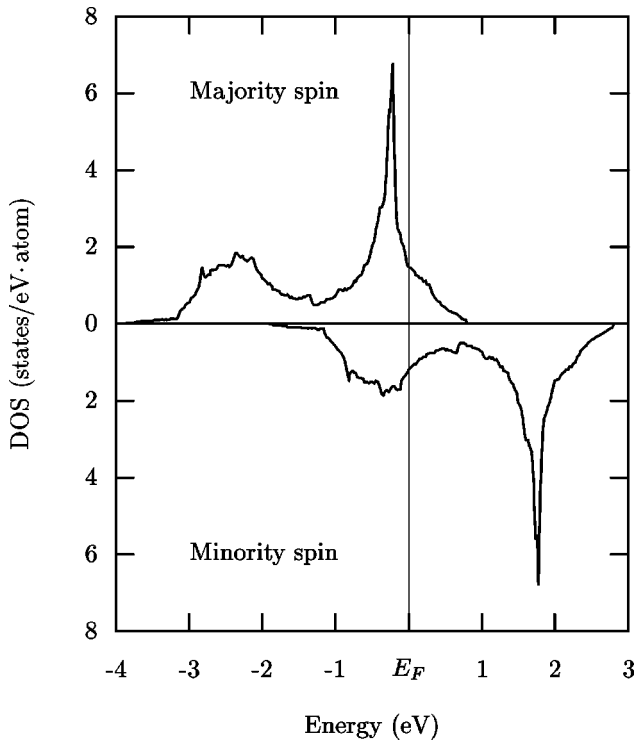

FIG. 1. The Fe majority- and minority-spin electron densities of states for our model, exhibiting the characteristic bonding and antibonding regions. Bandwidth is 4.7 eV and exchange splitting 2 eV.

fith's prescription,[32] and a lattice constant $a=2.87$ Å.[33] We have, thus, a five-band model. The bandwidth was set to 4.7 eV, which corresponds roughly to the bandwidth of d electrons in Fe.[34] The exchange-splitting energy Δ was chosen to be 2 eV, taking as reference the position of the peaks in the densities of states for majority and minority spins. Then, the Fermi level was fixed by the condition of having six electrons per unit cell. We show the density of states for majority and minority spins in Fig. 1. These exhibit the bonding and antibonding regions common to bcc materials with unfilled d shells. Once the Fermi energy is fixed, we can deduce the strength of the effective Coulomb interaction U in our model from $U=\Delta/(\langle n_\uparrow\rangle-\langle n_\downarrow\rangle)$. We find $U=0.69$ eV, which compares very well with the energy found in other works.[35] On the other hand, bulk polarization is too high, roughly 48%,[36] reflecting the lack of hybridization with sp electrons.

In a typical SPEELS experiment, the incoming electron beam impinges on the sample surface at an angle θ to the normal, and the total scattering angle is 90°.[11–13,22,23] For fixed scattering angle, i.e., for given incoming and outgoing momenta, there are three possible scattering processes corresponding to different momentum transfer. In two cases, an elastic (or specular) scattering event precedes or follows a relatively small-angle inelastic scattering event, giving momentum transfers $\mathbf{q}$ and $\mathbf{q}'$, respectively. In the third process, there is a single large-angle inelastic scattering event with a momentum transfer $\mathbf{q}''$ absorbed by the electron-hole pair excitations. We consider here the geometry of Venus and Kirschner,[12] that is, the sample exposes the (110) surface, and the scattering plane is defined by the surface normal [110] and the [001] axis. If u is the axis normal to the surface, the three momenta mentioned are given as a function of energy loss E, and impinging momentum p_i and energy E_i by

$$\begin{aligned} q_u &= p_i(\cos\theta-\sin\theta\sqrt{1-E/E_i}),\\ q_u' &= p_i(-\cos\theta+\sin\theta\sqrt{1-E/E_i}),\\ q_u'' &= -p_i(\cos\theta+\sin\theta\sqrt{1-E/E_i}),\\ q_z &= q_z'=q_z''=p_i(\sin\theta-\cos\theta\sqrt{1-E/E_i}). \end{aligned} \tag{3.1}$$

Momentum transfer parallel to the surface is the same in the three cases. To calculate the final spectrum, the contributions of these three processes have to be added because experiment does not discriminate between them.

Also, Fe, like the other transition element ferromagnets, presents a low but non-negligible density of freelike s and p states at the Fermi surface. Hence, the interaction between the incoming electrons and those in the solid will be screened. We take this into account using the Thomas-Fermi form of the screened Coulomb interaction $v(r)=(e^2/r)\exp(-q_{\mathrm{TF}}r)$ in Eq. (2.3) and $v(q)=4\pi e^2/(q^2+q_{\mathrm{TF}}^2)$ in Eq. (2.6), with a screening wave vector corresponding to the density of states of s and p electrons at the Fermi surface.[37] This gives $q_{\mathrm{TF}}=0.26$ in units of $k_a=4\pi/a$. Finally, we use a finite value for η when taking the analytic continuation $i\omega_n\rightarrow E+i\eta$. Since, to our knowledge, there are no estimates of the self-energy corrections[38] for the case of Fe, we take $\eta=80$ meV, which corresponds to the resolution in the latest experiment on this material.[20]

A. Interband densities of Stoner states

Let us consider an incoming majority-spin electron with an angle of incidence $\theta=60°$ to the normal and energy $E_i=22$ eV, which is the energy used in Ref. 12. We see in Fig. 2(a) that the total spin-flip exchange scattering cross section is indeed rather broad, with its peak centered at an energy much higher than the exchange-splitting value (2 eV in our model), a trend observed experimentally by Venus and Kirschner.[12] We also show the partial cross sections for different momentum transfers. The curves for the small scattering angle coincide for symmetry reasons. Though total cross-section broadness is somewhat increased because of the difference between small-angle and large-angle scattering, the cross section in each case is broad in itself. We have examined the origin of the structure in this spectrum. First, we separated Stoner excitations and many-body effects. In Fig. 2(b) we show the noninteracting cross section, given by the Stoner term of the response function in Eq. (2.10), and the interacting cross section, given by the full response function, including the many-body term. This figure clearly shows us the contributions of collective modes. Indeed, the broad feature starting around 0.2 eV indicates the excitation low-lying spin waves, and, more interestingly, the shoulder below 2 eV indicates the excitation of high-energy spin

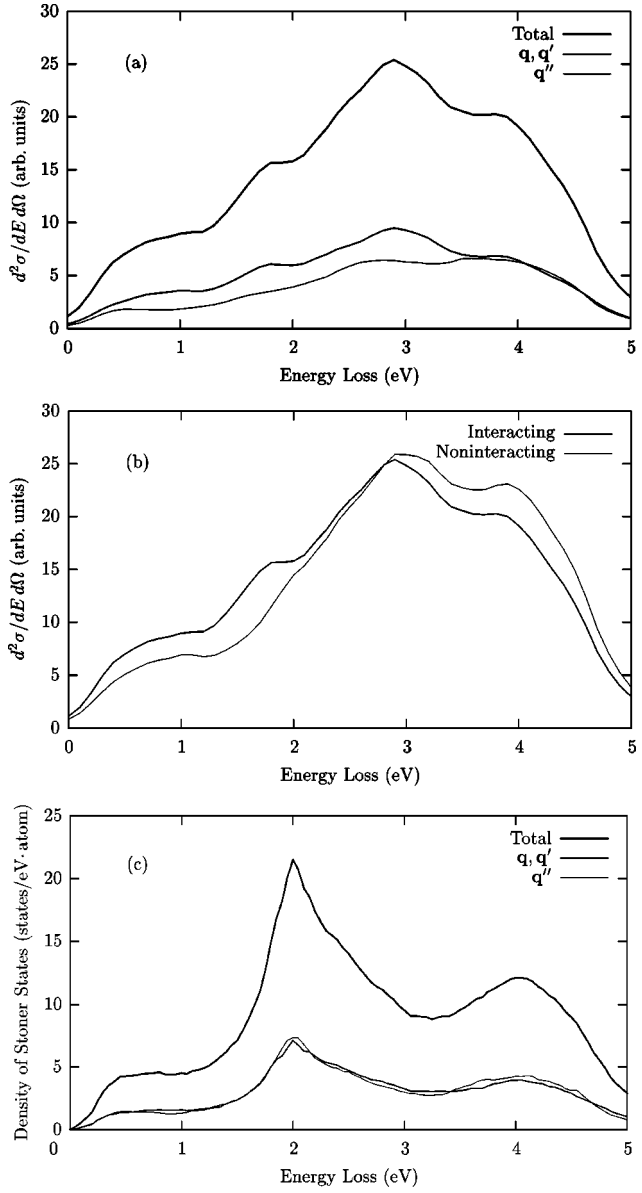

FIG. 2. (a) Spin-flip exchange cross section for a majority-spin electron, with impinging energy of 22 eV and angle of incidence of 60°. We show the total cross section, as well as the partial cross sections for different momentum transfer. The peak is at 3 eV, an energy much higher than the exchange-splitting energy $\Delta=2$ eV. (b) Interacting and noninteracting cross sections. The difference between both curves clearly shows two collective modes, one just below 2 eV, and the other below 1 eV. The noninteracting cross section shows three distinct features, namely, the peak at 3 eV, a shoulder at 4 eV, and a broad hump around 1 eV. (c) The total and partial densities of Stoner states. These show the typical maxima at the exchange splitting energy, which are absent from the SPEELS spectrum. The densities of Stoner states are incapable of explaining the peak of the SPEELS spectrum at 3 eV.

waves. This is important because these so-called ''optical'' spin waves[39] have not been discussed previously in connection with SPEELS measurements. A detailed plot of the many-body contributions to the cross section shows that the low-lying spin wave peaks around 0.4 eV, while the high-energy spin wave peaks around 1.65 eV. We consider spin waves again further on, and we concentrate here on the single-particle traits. Besides the peak at 3 eV, the noninteracting cross section shows a shoulder at 4 eV and a broad feature, albeit much smaller, at low-energy loss, around 1 eV or so. SPEELS spectra have often been interpreted in terms of the density of Stoner states. Accordingly, we show in Fig. 2(c) the total density of Stoner states, as well as the densities of Stoner states for different momentum transfer (as before, the curves for small-angle scattering are the same).[40] It is evident in the cross sections that there is nothing reminiscent of the high density of Stoner states at the exchange-splitting energy. The only features of the cross sections that can find an explanation in the density of Stoner states are the shoulder at 4 eV and, possibly, the hump around 1 eV. We have, thus, refined our study and have considered the behavior of the density of Stoner states as a function of energy loss and the bands coupled in an excitation [recall energy loss and momentum transfer are coupled, cf. Eq. (3.1)]

$$\rho_{nn'}(E)=\frac{1}{N_0}\sum_{\mathbf{k}}\,(f_{n'\mathbf{k}-\mathbf{q}\sigma_f}-f_{n\mathbf{k}\sigma_i})\times\delta(E+\epsilon_{n'\sigma_f}(\mathbf{k}-\mathbf{q})-\epsilon_{n\sigma_i}(\mathbf{k})). \tag{3.2}$$

Hence, subscripts n and n' indicate minority and majority bands, respectively (bands are numbered from bottom to top). We show a plot of the density of states thus defined in Fig. 3(a). We can see that the possible interband excitations are completely identified. Moreover, the series of Stoner peaks clearly reflects the bonding and antibonding nature of the electronic structure, giving rise to two arrays of peaks, for higher and lower excitation energies.[41] The question is, of course, which of these Stoner peaks contributes the most to SPEELS cross sections. The answer is to be found, perhaps unsurprisingly, in how strongly the different bands are coupled by the matrix elements $W_{nn'}$ of the electron-hole creation operator. What is not so obvious is the outcome of the combined effect of Stoner peaks and matrix elements. Let us consider the average value of $|W_{nn'}|^2$ over the Brillouin zone:

$$\langle|W_{nn'}|^2\rangle=\frac{1}{\hat{v}}\sum_{\mathbf{k}}\,|W_{nn'}|^2 \tag{3.3}$$

($\hat{v}$ denoting the volume of the Brillouin zone). In Fig. 3(b) we show the graph of $\langle|W_{nn'}|^2\rangle$ as a function of energy loss and of bands coupled. There is little significant variation as a function of energy loss, but a very important structure as a function of band couple, resulting in a wavelike pattern. Comparing Figs. 3(a) and 3(b), we can clearly see when it is that both quantities, $\rho_{nn'}$ and $\langle|W_{nn'}|^2\rangle$, interfere constructively. Thus, although the density of Stoner states reaches is highest peak at exchange splitting, the average $\langle|W_{nn'}|^2\rangle$ is negligible for the corresponding band couples. Instead, although the densities of Stoner states for interband excitations 21 and 22, 31 and 32, and 41 and 42 are more modest, the corresponding matrix element averages are high, whence the peak around 3 eV and the shoulder around 4 eV in the non-

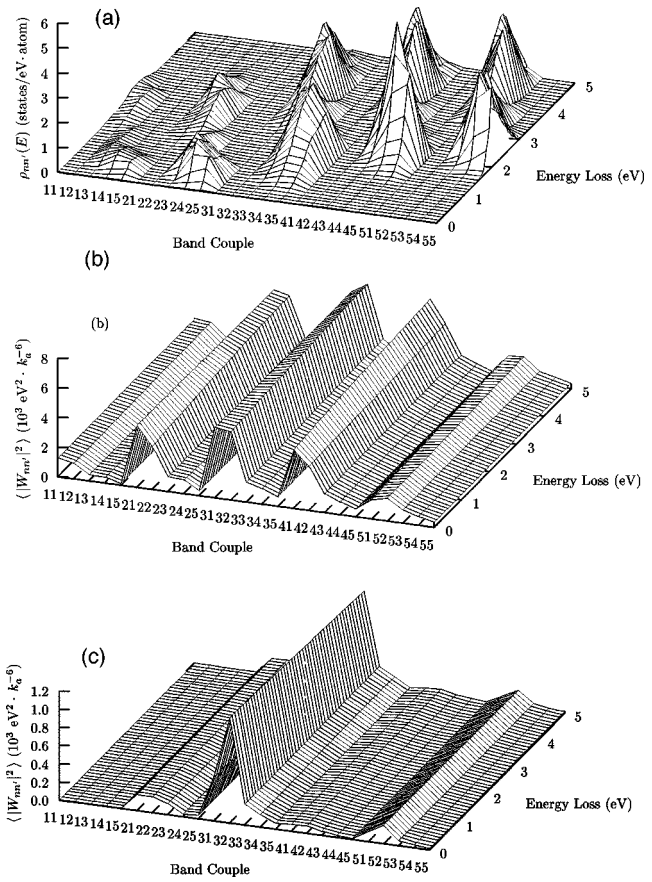

FIG. 3. (a) Three-dimensional (3D) plot of the interband densities of Stoner states. The possible interband excitations are clearly identified. The two series of peaks reflect the bonding and antibonding nature of the Fe electronic structure. The highest peak is found at exchange splitting, for $nn'=44$. As we explain in the text, however, this peak contributes little to the spin-flip exchange cross section. (b) 3D plot of the average $\langle|W_{nn'}|^2\rangle$. The slight dependence on energy results in the wavelike form of the surface. The lines on the surface parallel to the energy axis correspond to fixed band couple value. The important interband excitations are determined by the crests, namely, 21, 22, 31, 32, 41, and 42. One can also observe that $\langle|W_{nn'}|^2\rangle$ reaches its lowest values for $nn'=15,\ldots,55$. (c) 3D plot of $\langle|W_{nm}|^2\rangle$ without umklapp processes, The important interband excitations have been reduced to $nn'=31,32$, thus singling out excitations in a restricted energy range.

interacting cross section in Fig. 2(b). Actually, the peak at 3 eV is more of a hat on top of the high cross-section value due to interband excitations 31 and 32. We can also see that the hump around 1 eV is due to excitations coupling bands 2 and 3, and 2 and 4. To corroborate our analysis, we show in Fig. 4 the cross section taking into account solely the interband processes mentioned above. We include the total noninteracting cross section for comparison as well. We see that the few interband excitations considered indeed account almost completely for the structure of the noninteracting spectrum. An argument to understand how so simple a picture can work is that, since the atomic $3d$ orbitals are localized, their Fourier transform is rather flat, so that $|W_{nn'}|^2$ in the single-particle correlation function $\chi^{S}_{\sigma_i\sigma_f}$ [cf. Eq. (2.11)] may be

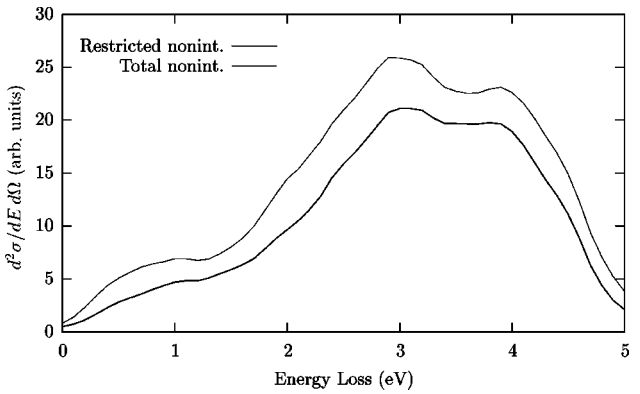

FIG. 4. The noninteracting scattering cross section taking into account only 8 ($nn'=21,22,23,24,31,32,41,42$) out of the 25 possible interband excitations, selected as explained in the text, compared to the total noninteracting scattering cross section. The first curve follows the second one very closely.

replaced by its average value over the Brillouin zone. Thus, $\chi^{S}_{\sigma_i\sigma_f}$ is approximately proportional to $\Sigma_{nn'}\rho_{nn'}\langle|W_{nn'}|^2\rangle$, a weighted average of the interband densities of Stoner states.

B. Umklapp processes

Another most interesting phenomenon playing a fundamental role in SPEELS is umklapp scattering. One can see in Eq. (2.6) that the contribution of umklapp processes ($\mathbf{K}\neq 0$) to the particle-hole excitation operator $\varrho_{\sigma_i\sigma_f}$ is weighted by the Coulomb interaction and the Wannier wave functions. Because of the decay of the Coulomb potential as well as of the atomic orbitals with increasing wave vector, the weight becomes rapidly negligible for reciprocal lattice vectors beyond first-nearest neighbors. This is enough, however, for umklapp processes to have a twofold effect. To see this, let us consider cross sections, taking into account only normal excitations (i.e., with respect to the first Brillouin zone). We show this in Fig. 5, where we plot both the interacting and noninteracting no-umklapp cross sections. First,

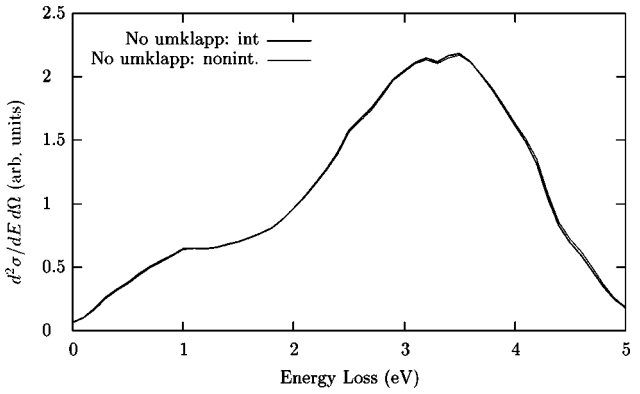

FIG. 5. Spin-flip exchange scattering cross section without umklapp processes. All that is left is a broad maximum between 3 and 4 eV, and a hump at 1 eV. Clearly, the most important information is lost, i.e., the peak at 3 eV and the shoulder at 4 eV. Also, all trace of spin waves in the spectrum has disappeared [cf. Fig. 2(b)].

we see that, quite apart from their much lower values in comparison with the response taking into account umklapp scattering, spectra in Fig. 5 show little resemblance with those in Fig. 2(b) (the scale in both figures is the same). This is because the possible interband excitations have been drastically reduced. Indeed, let us consider the graph of the average $\langle |W_{nn'}|^2 \rangle$ for excitations strictly conserving crystal momentum. We show this in Fig. 3(c). The wave crests have been reduced to that for $nn' = 31,32$, from which it is obvious that the different wave crests in Fig. 3(b) are due to umklapp scattering. Normal scattering alone results in a spectrum almost completely distorted because of the excitation of interband transitions mainly for energies between 3 and 4 eV [cf. Fig. 3(a)].

Furthermore, in Fig. 5 it is immediately apparent that there remains no trace of spin waves in the spectrum. Indeed, the interacting and noninteracting curves are almost indistinguishable, with no hint of any collective mode. At this point it is important to consider the behavior of the low-lying spin wave for small wave vector because of its indication of the stability of the ground state. We have calculated the low-lying spin-wave dispersion relation and found it tends linearly to 218.7 meV for $q \rightarrow 0$. The slope is low but positive, with a value of 8.9 meV Å. Thus our model is consistent. However, we cannot expect from it further predictive power regarding spin waves. For instance, we see our low-lying mode is technically an ''optical'' mode, and not an ''acoustic'' mode, as expected. The reason is that the energy bands in our model are purely *d*. It is well known that models of itinerant ferromagnetism that do not take into account hybridization with *sp* bands fail to yield appropriate dispersion relations for spin waves.[42] Thus, our high-energy mode is much too high compared to the neutron scattering results of Perring *et al.*[9] Nevertheless, we do think our results properly introduce high-energy spin waves as a source of structure in SPEELS measurements, pointing to umklapp scattering as the mechanism for their excitation.

IV. DISCUSSION

We wish to discuss some of the issues considered in this work pertaining to other theoretical and experimental findings. First of all, as we have shown [cf. Fig. 2(b)], the maximum in the SPEELS spectrum does not necessarily correspond to the exchange-splitting energy of the ferromagnet, since the peak in the spectrum is at 3 eV and $\Delta = 2$ eV in our model. Thus, the common assumption that this peak allows us to estimate the magnetic moment[22,23] through its correlation with exchange splitting should be reconsidered, both in bulk and surface studies.

Also, the broadness of the spectrum is generally associated with a nonconstant exchange splitting over the Brillouin zone (see, e.g., Ref. 11). While we agree a nonconstant exchange splitting will have this effect, we have seen that a most important source of broadness is umklapp scattering, together with the structure of the interband densities of Stoner states of the material. As mentioned in the Introduction, Venus and Kirschner[12] intended to correlate the behavior of the Stoner peak with varying scattering angle with that of the peak in the total density of Stoner states. According to our results, this picture is not correct. The maximum in the spectrum depends on the relative weight of a few interband densities of Stoner states, which is determined by the matrix elements for such excitations. In this respect, a calculation of the interband densities of Stoner states and of the weights $W_{nn'}$ employing accurate electronic bands and wave functions would be most clarifying. To allow for a closer comparison with theory, it would be desirable to have experimental results of the Stoner region of the SPEELS spectrum with improved resolution, particularly in the case of Fe (for which the only available results are still those of Ref. 12, whose resolution is of only 400 meV).

Abraham and Hopster interpret the onset of Stoner excitations found in their work in terms of the $3d$ band structure of Ni.[13] This could readily be verified having at hand the interband densities of Stoner states for this material. Indeed, these authors consider in particular interband excitations corresponding to $nn' = 55$, the onset of which, if they exist, could be easily identified in a graph like that in Fig. 3(a). A point still to be verified would be if the matrix elements for such excitations are sufficiently important. Furthermore, the little difference of spectra for 10°, 20°, and 40° off specular scattering angles reported by these authors would mean that the interband densities of Stoner states and umklapp weights differ little for those angles in the case of Ni. Thus, a theoretical calculation along the lines in our work would help us understand better the Stoner spectrum of this material.

Spin waves, both acoustic and optical, have long been predicted in itinerant ferromagnets and subsequently observed in neutron scattering experiments.[1,4,28,30] The first detection of the acoustic mode in Fe in a SPEELS experiment has also been reported recently.[20] Our work poses the question of the possibility of observing in SPEELS measurements the optical modes as well. The question to be studied in the future is if there can be enough coupling between the incoming electron and those in the solid to excite an optical spin wave. According to our model, it is umklapp processes that provide the necessary coupling to excite the high-energy spin waves. This is consistent with the picture of Cooke and coworkers that these modes derive from interband transitions.[29] We would expect the high-energy modes to be observed in SPEELS experiments on Ni, since it is a strong ferromagnet, allowing for well-defined spin waves. The case of Fe appears to be more problematical, since it is a weak ferromagnet. Indeed, theoretical studies of the dynamical susceptibility by Tang, Plihal, and Mills[8] and by Savrasov[43] fail to predict any high-energy spin wave in the case of Fe. On the other hand, these results are at odds with similar investigations by Cooke and co-workers.[29] They seem to be also at odds with the experimental findings of Perring *et al.*[9] and of Paul *et al.*[44] Whether the experimental findings in the case of Fe can be explained in terms of Stoner excitations is an open question.[45] Our present calculation, with parameters corresponding to Fe, does predict the observation of the high-energy spin waves in SPEELS measurements. It could be, however, that acoustic spin waves, when present, drain most of the oscillator strength. This is plausible because it is

known that acoustic spin waves in Fe arise upon hybridization of *d* electrons with *sp* electrons. Matrix elements (i.e., umklapp couplings) with *sp* hybridization will be more important because of the larger extension and magnitude of the 4*s* wave functions. This implies, of course, as our model does, that optical modes are mainly *d* in character. (The case of Ni appears to be different, since even a pure *d* band model of Ni shows acoustic spin waves.[5])

The analysis presented in this work can prove useful more broadly in the understanding of ferromagnetism. Recently, Hirsch has presented a model of ferromagnetism without exchange splitting, in which spin polarization arises upon broadening of the majority-spin bands relative to the minority-spin bands.[46] If this mechanism plays an important role in itinerant ferromagnets, then the interband densities of Stoner states will change considerably because pairs of bands other than those in the Stoner picture of ferromagnetism will be involved. Consequently, the predicted exchange scattering spectra will be different in both pictures. Thus, SPEELS can prove a useful tool to validate or disprove Hirsch's model.

Finally, we comment on the question of whether bulk or surface properties are measured by SPEELS. Our calculations here have focused on bulk properties. However, some authors have presented SPEELS as a technique more appropriate for surface studies.[23,25] The reason for concern is the mean free path of electrons at the energies used in SPEELS. Experimental estimates for Fe films give values between 5 Å and 7 Å, depending on the crystal direction and nature of the substrate[47] for electrons with an energy of 20 eV. The question raised, however, is not simple and requires more detailed consideration, both theoretically and experimentally. Still, most of the observations to date have been discussed in the light of bulk calculations.[12,13,20] In this regard, a recent report on the electron dynamics at the surfaces of noble metals (Ag and Cu) is appropriate to mention. Bürgi *et al.*[48] have found that the dynamics of hot electrons at surfaces can be dominated by bulk electrons. This offers more support to the premise that our results offer a sensible explanation for SPEELS results.

V. SUMMARY AND CONCLUSIONS

In this work we address the problem of the interpretation of the SPEELS spectrum of itinerant ferromagnets. We find that considerably more information can be drawn from these measurements than has been recognized until now. We have found that the peaks of the spectra in the Stoner region are the image of a few interband densities of Stoner states of the material. These are very sensitive to the electronic structure of the material and illustrate very clearly the possible interband excitations. Which are the most significant interband excitations is determined by the couples of bands singled out by the average weight over the Brillouin zone of the squared matrix elements for the corresponding Stoner excitations. In this respect, umklapp processes play a most fundamental role. Our model also predicts that high-energy spin waves should be excited in SPEELS experiments, with umklapp scattering providing the necessary coupling. Our results allow us to explain several of the features observed in SPEELS spectra, suggesting a mechanism for the electronic excitations involved in these experiments. From the theoretical point of view, *ab initio* calculations of the interband densities of Stoner states and matrix elements $W_{nn'}$ would provide a closer look at the elementary excitations in itinerant ferromagnets. The differences between different ferromagnets, like Fe and Ni, could also be better understood. From the experimental point of view, measurements with higher resolution would be desirable, both for the study of the Stoner region and of spin waves. We think our results provide a good starting point for those further studies.

ACKNOWLEDGMENTS

R.S. would like to thank the members of the Department of Applied Physics at Chalmers University of Technology for their hospitality during a stay in which part of this work was done. This project was supported by the Swedish Natural Science Research Council. R.S. would also like to thank Suk Joo Youn and Ove Jepsen for linear muffin-tin orbital–atomic sphere approximation (LMTO-ASA) data for Fe, and Anthony Paxton for providing him with useful literature. Many thanks in particular to Professor A. J. Freeman for encouraging discussions.

[1] R. Kubo, T. Izuyama, D. J. Kim, and Y. Nagaoka, J. Phys. Soc. Jpn. **17**, Suppl. B-I, 67 (1962); T. Izuyama, D. J. Kim, and R. Kubo, *ibid.* **18**, 1025 (1963).
[2] C. Herring, in *Magnetism*, edited by G. T. Rado and H. Suhl (Academic Press, New York, 1966), Vol. IV.
[3] H. A. Mook, R. M. Nicklow, E. D. Thompson, and M. K. Wilkinson, J. Appl. Phys. **40**, 1450 (1969).
[4] H. A. Mook and R. M. Nicklow, Phys. Rev. B **1**, 336 (1973).
[5] R. D. Lowde and C. G. Windsor, Adv. Phys. **19**, 813 (1970).
[6] J. F. Cooke, Phys. Rev. B **7**, 1108 (1973).
[7] J. F. Cooke, J. W. Lynn, and H. L. Davis, Phys. Rev. B **21**, 4118 (1980).
[8] H. Tang, M. Plihal, and D. L. Mills, J. Magn. Magn. Mater. **187**, 23 (1998).
[9] T. G. Perring, A. T. Boothroyd, D. McK. Paul, A. D. Taylor, R. Osborn, R. J. Newport, J. A. Blackman, and H. A. Mook, J. Appl. Phys. **69**, 6219 (1991).
[10] H. Hopster, R. Raue, and R. Clauberg, Phys. Rev. Lett. **53**, 695 (1984).
[11] J. Kirschner, D. Rebenstorff, and H. Ibach, Phys. Rev. Lett. **53**, 698 (1984).
[12] D. Venus and J. Kirschner, Phys. Rev. B **37**, 2199 (1988).
[13] D. L. Abraham and H. Hopster, Phys. Rev. Lett. **62**, 1157 (1989).
[14] S. Yin and E. Tosatti, ICTP, Report No. IC/81/129 (unpublished).
[15] J. Glazer and E. Tosatti, Solid State Commun. **52**, 905 (1984).
[16] G. Vignale and K. S. Singwi, Phys. Rev. B **32**, 2824 (1985).
[17] C. J. Bocchetta, E. Tosatti, and S. Yin, Z. Phys. B: Condens. Matter **67**, 89 (1987).

[18] R. Saniz and S. P. Apell, Phys. Rev. B **48**, 3206 (1993).
[19] M. Plihal and D. L. Mills, Phys. Rev. B **58**, 14 407 (1998).
[20] M. Plihal, D. L. Mills, and J. Kirschner, Phys. Rev. Lett. **82**, 2579 (1999).
[21] J. Kirschner and J. Hartung, Vacuum **41**, 491 (1990).
[22] T. G. Walker, A. W. Pang, H. Hopster, and S. F. Alvarado, Phys. Rev. Lett. **69**, 1121 (1992).
[23] H. Hopster, Surf. Rev. Lett. **1**, 89 (1994).
[24] M. P. Gokhale, A. Ormeci, and D. L. Mills, Phys. Rev. B **46**, 8978 (1992).
[25] M. P. Gokhale and D. L. Mills, Phys. Rev. B **49**, 3880 (1994).
[26] M. Plihal and D. L. Mills, Phys. Rev. B **52**, 12 813 (1995).
[27] A similar claim was made in Ref. 11.
[28] J. F. Cooke, J. A. Blackman, and T. Morgan, Phys. Rev. Lett. **54**, 718 (1985).
[29] J. A. Blackman, T. Morgan, and J. F. Cooke, Phys. Rev. Lett. **55**, 2814 (1985).
[30] H. A. Mook and D. McK. Paul, Phys. Rev. Lett. **54**, 227 (1985).
[31] A. L. Fetter and J. D. Walecka, *Quantum Theory of Many-Particle Systems* (McGraw-Hill, New York, 1971).
[32] J. S. Griffith, *The Theory of Transition-Metal Ions* (Cambridge University Press, Cambridge, 1961).
[33] N. W. Ashcroft and N. D. Mermin, *Solid State Physics* (Saunders College, Philadelphia, 1976).
[34] This is a full potential linear muffin-tin orbital (FPLMTO) estimate of the majority *d*-band width for Fe at the *H* point. R. Saniz (unpublished).
[35] The value of the effective intra-atomic Coulomb interaction is found to be around 0.5 to 1 eV for all transition metals. See E. P. Wohlfarth, in *Ferromagnetic Materials* (North-Holland, Amsterdam, 1980), Vol. 1. See also G. Tréglia, F. Ducastelle, and D. Spanjaard, J. Phys. **43**, 341 (1982), and M. M. Steiner, R. C. Albers, and L. J. Sham, Phys. Rev. B **45**, 13 272 (1992).
[36] An LMTO-ASA estimation gives approximately 36% for the polarization of *d* electrons. S. J. Youn (private communication).
[37] The LMTO-ASA value is roughly 0.09 states/eV atom. S. J. Youn and O. Jepsen (private communication).
[38] Interesting references in the case of Ni for this difficult question are H. I. Starnberg and P. O. Nilsson, J. Phys. F: Met. Phys. **18**, L247 (1988), and F. Aryasetiawan, Phys. Rev. B **46**, 13 051 (1992). See also F. Aryasetiawan and O. Gunnarson, Rep. Prog. Phys. **61**, 237 (1998) for a more general discussion.
[39] The term ''optical'' spin wave was first introduced, to our knowledge, by Cooke and collaborators in Ref. 7 to refer to the high-energy spin-wave modes they found in their dynamical susceptibility studies of Ni and Fe. They also used the term ''acoustic'' to refer to the well-known low-lying spin wave with quadratic behavior for small momentum.
[40] Note that the densities of Stoner states do not quite vanish for zero energy loss. For off specular scattering, $E=0$ corresponds to elastic scattering with finite momentum transfer, which presents a low, but finite, density of Stoner states.
[41] Indeed, it is not difficult to see that for $n=3,4,5$ the Stoner peaks correspond essentially to excitations coupling (minority) antibonding holes to (majority) antibonding electrons, for lower energy cases, and to bonding electrons for higher energy. The same is true for the coupling of the $n=1,2$ bonding holes with electrons.
[42] See R. B. Muniz, J. F. Cooke, and D. M. Edwards, J. Phys. F: Met. Phys. **15**, 2357 (1985). It is also shown in this paper that a proper introduction of sp hybridization causes the low-lying mode to become acoustic.
[43] S. Y. Savrasov, Phys. Rev. Lett. **81**, 2570 (1998).
[44] D. McK. Paul, P. W. Mitchell, H. A. Mook, and U. Steinberger, Phys. Rev. B **38**, 580 (1988).
[45] The SPEELS calculations of Plihal and Mills show no high-energy spin waves either, but all indicates that these authors did not include umklapp processes in their work. See Ref. 19.
[46] J. E. Hirsch, Phys. Rev. B **59**, 6256 (1999).
[47] A. Hopster, J. Electron Spectrosc. Relat. Phenom. **98**, 17 (1999).
[48] L. Bürgi, O. Jeandupeux, H. Brune, and K. Kern, Phys. Rev. Lett. **82**, 4516 (1999).